Supporting Information

Scanning Electrochemical Microscopy of Individual Single-Walled Carbon Nanotube

Jiyeon Kim,[†] Hui Xiong,[†,¶] Mario Hofmann,[§] Jing Kong,[§] and Shigeru Amemiya[†,*]

[†] *Department of Chemistry, University of Pittsburgh, Pittsburgh, Pennsylvania 15260, and*

[§] *Department of Electrical Engineering and Computer Science, Massachusetts Institute of Technology, Cambridge, Massachusetts 02139.*

[¶] Present address: Energy Systems Division, Argonne National Laboratory, Argonne, IL, 60439

* To whom correspondence should be addressed. E-mail: amemiya@pitt.edu.

Chemicals. Ferrocenylmethyltrimethylammonium hexafluorophosphate, $FcTMAPF_6$, was prepared by the metathesis of ferrocenylmethyltrimethylammonium iodide (Strem Chemical, Newburyport, MA) and ammonium hexafluorophosphate (Strem Chemical). A 0.1 KNO_3 solution containing 0.3 mM $FcTMAPF_6$ was prepared with 18.3 MΩ·cm deionized water (Nanopure, Barnstead, Dubuque, IA).

SECM Measurements. SECM experiments were conducted by employing a commercial SECM instrument with closed-loop piezoelectric motors (CHI 910B, CH Instruments, Austin, TX, USA) to control the position of a Pt disk probe at nanometer scale. A 1.5 μm-diameter probe with RG = 2 (= r_g/a; r_g is the outer tip radius) was fabricated by milling the tip of a glass-insulated Pt wire using a focused ion beam technique (SMI3050SE FIB-SEM, Seiko Instruments, Chiba, Japan). The tip fabrication will be described in the details of a future paper. A 10 μm-diameter probe with RG = 10 was purchased from CH Instruments. The inner and outer tip radii of the respective probes were checked by SEM and optical microscopy and then determined from current approach curves at a glass substrate.[S1, 2] A 1 mm-diameter AgCl-coated Ag wire served as a reference/counter electrode. A SWNT sample was placed in a two-electrode cell such that the longest axis of the SWNTs is parallel to the *y*-direction of the piezoelectric motor (Figure 1). The substrate surface was aligned vertically with respect to the length of the tip so that a constant tip current was obtained when the tip was scanned above the surrounding SiO_2 surface in *x*- and *y*-directions at a constant height. The *x*- and *y*- positions of the SWNT with respect to the edges of the substrate were determined by SEM (Figure 2) so that the same SWNT can be studied using different probes.

Location of a SWNT. SECM allows for location of an individual SWNT with precision of ± 100 nm when a 1.5 μm-diameter probe is employed (Figure S1).

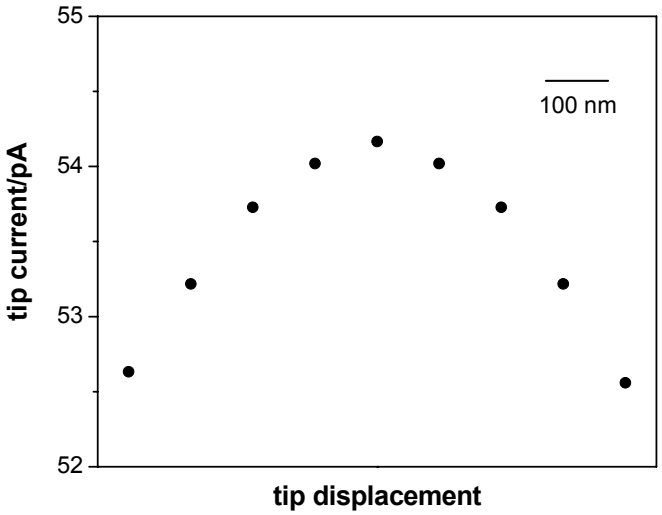

Figure S1. The peak current as obtained by magnifying the SECM line scan at the second from the left-hand side in Figure 4a. Each data point was obtained at every 100 nm.

Accessibility of the Sidewall of an Individual SWNT. Here we demonstrate that uniform accessibility of the SWNT sidewall is a good approximation in eq 2 when mediator regeneration at the sidewall is kinetically limited. Specifically, we assess distribution of normal flux of mediator molecules at the sidewall of an individual SWNT. A model proposed by Macpherson and co-workers[S3] (Figure S2) was used to reduce the problem to 2D diffusion in the *x*,*z*-plane (see Figure 1 for definition of *x*- and *z*-axes). The width of the gap between the SECM tip and an insulating substrate with a SWNT is comparable to the tip radius, *a*, which is much larger than the nanotube radius, *r* (*a* > 1000*r* in Figure S2).

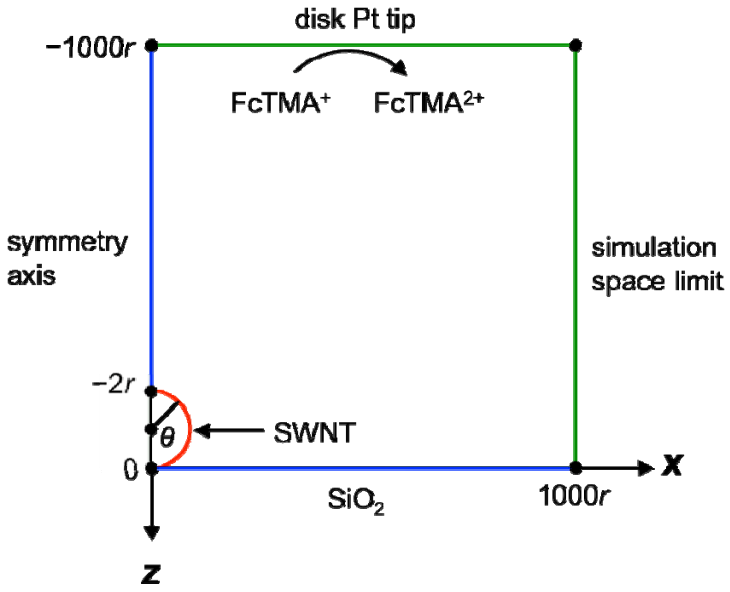

Figure S2. Geometry of the SECM diffusion problem in the Cartesian coordinate. There is no normal flux at blue lines while mediator concentration is equal to a bulk concentration at the green lines.

Diffusion of a tip-generated species, $FcTMA^{2+}$, in the gap reaches a steady state as defined by

$$D\left[\frac{\partial^2 c(x,z)}{\partial x^2}+\frac{\partial^2 c(x,z)}{\partial z^2}\right]=0 \qquad \text{(S1)}$$

where $c(x, z)$ is the concentration of $FcTMA^{2+}$. The boundary condition at the SWNT sidewall is given by

$$J(\theta)=k_{et}c(\theta) \qquad 0\le\theta\le\pi/2 \qquad \text{(S2)}$$

with

$$\tan\theta = \frac{x}{z+r} \tag{S3}$$

where $J(\theta)$ and $c(\theta)$ are normal flux and concentration of $FcTMA^{2+}$ at the sidewall, respectively. The other boundary conditions are given in Figure S2. The simulation space limit is so far from the SWNT that the corresponding boundary condition is determined by the tip reaction to be identical with the boundary condition at the tip (see Figure 5b in ref. S4 for validation of this assumption).

The two-dimensional diffusion problem was solved using Comsol Multiphysics 3.5a (COMSOL, Inc., Burlington, MA) to calculate distribution of the normal flux of mediator molecules at the sidewall. Dimensionless parameters were used in the attached simulation file, where an electron transfer rate constant is given in the dimensionless form as

$$K = \frac{k_{et} r}{D} \tag{S4}$$

Figure S3 shows normalized flux, $J(\theta)/J(\theta = \pi)$, thus simulated for K = 10, 1, and 0.1. The respective K values correspond to k_{et} = 1000, 100, and 10 cm/s in eq S4 with $2r$ = 1.8 nm and D = 9.0×10^{-6} cm^2/s.

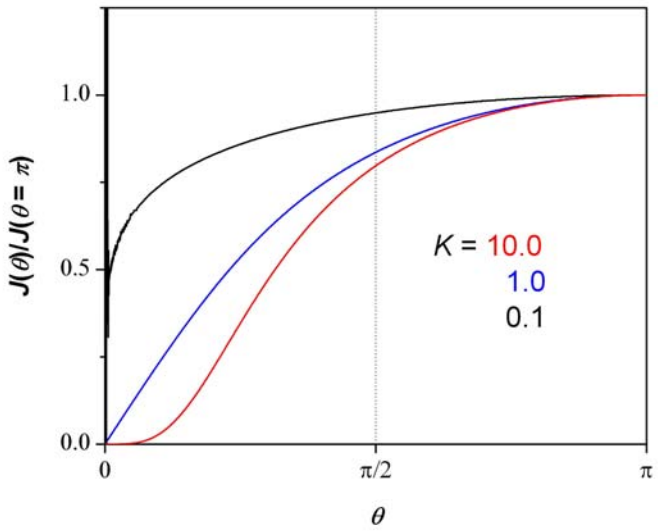

Figure S3. Simulated flux at the sidewall of an individual SWNT in the normalized form.

When electron transfer is diffusion limited (K = 10) or close to the diffusion limitation (K = 1), mediator regeneration occurs non-uniformly at the sidewall. In these cases, original mediators are efficiently regenerated at the top half of the sidewall, which is exposed to the gap to obtain large normalized flux of $J(\theta \geq \pi/2)/J(\theta = \pi) > 0.70$. At the same time, smaller flux is obtained at the bottom half of the sidewall ($\theta < \pi/2$), where access of redox molecules is blocked by the underlying insulating substrate. On the other hand, flux distribution is much more uniform with K = 0.1. Large normalized flux of $J(\theta)/J(\theta = \pi) > 0.50$ is achieved even at very small θ of 0.01π although the flux itself is small because of a kinetic limitation. This apparently uniform accessibility is due to slow mediator regeneration at the top half of the sidewall, where the tip-generated species are consumed slowly to diffuse to the bottom half.

Overall, eq 2 is a good approximation when mediator regeneration at the SWNT is kinetically limited. In this case, eq 2 is obtained from eq S2 using $c(\theta) \approx c_{SWNT}$ and $J(\theta)$ =

i_{SWNT}/nFA. The extremely large k_{et} value of 1000 cm/s is required for a diffusion limitation because of highly efficient mass transfer at the SWNT with a molecular scale diameter.[S5] This result suggests that mediator regeneration at the SWNT is kinetically limited. It should be noted that more precise determination of a rate constant requires numerical simulation of a three-dimensional diffusion problem at the SWNT under the SECM configuration. Such a simulation, however, is hampered by the large tip diameter with respect to the nanotube diameter in our measurements,[S4,S6] thereby requiring a smaller probe.

REFERENCES

(S1) Shao, Y.; Mirkin, M. V. *J. Phys. Chem. B* **1998**, *102*, 9915–9921.

(S2) Amemiya, S.; Bard, A. J. *Anal. Chem.* **2000**, *72*, 4940–4948.

(S3) Wilson, N. R.; Guille, M.; Dumitrescu, I.; Fernandez, V. R.; Rudd, N. C.; Williams, C. G.; Unwin, P. R.; Macpherson, J. V. *Anal. Chem.* **2006**, *78*, 7006–7015.

(S4) Xiong, H.; Gross, D. A.; Guo, J.; Amemiya, S. *Anal. Chem.* **2006**, *78*, 1946–1957.

(S5) Heller, I.; Kong, J.; Heering, H. A.; Williams, K. A.; Lemay, S. G.; Dekker, C. *Nano Lett.* **2005**, *5*, 137–142.

(S6) Xiong, H.; Kim, J.; Kim, E.; Amemiya, S. *J. Electroanal. Chem.* **2009**, *629*, 78–86.

COMSOL Model Report

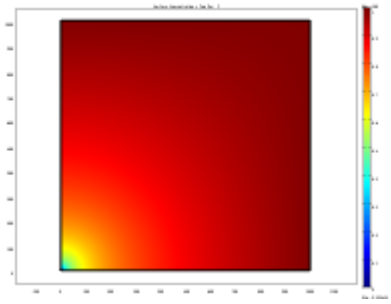

1. Table of Contents

2. Model Properties

Property	Value
Model name	
Author	
Company	
Department	
Reference	
URL	
Saved date	Oct 8, 2009 3:33:02 PM

Creation date	Oct 7, 2009 3:38:37 PM
COMSOL version	COMSOL 3.5.0.608

File name: C:\SWNT.mph

Application modes and modules used in this model:

- Geom1 (2D)
  - Diffusion (Chemical Engineering Module)

3. Geometry

Number of geometries: 1

3.1. Geom1

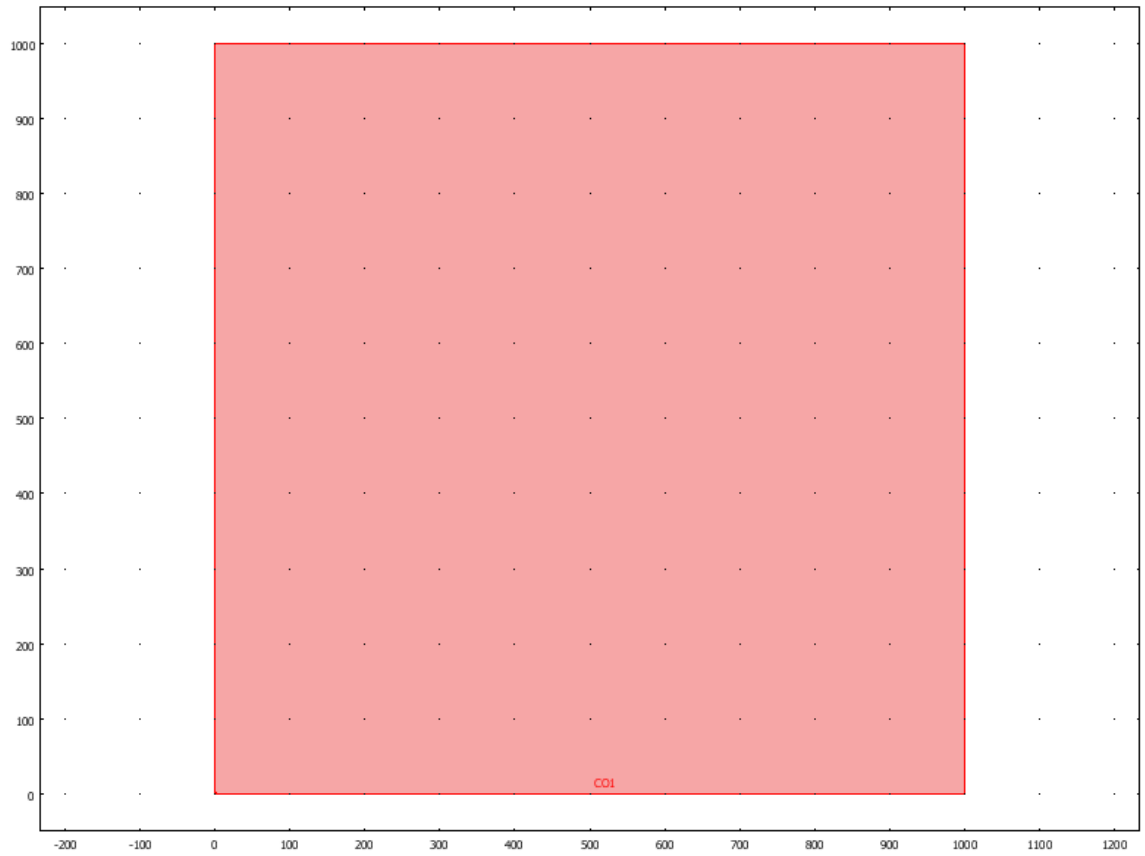

3.1.1. Point mode

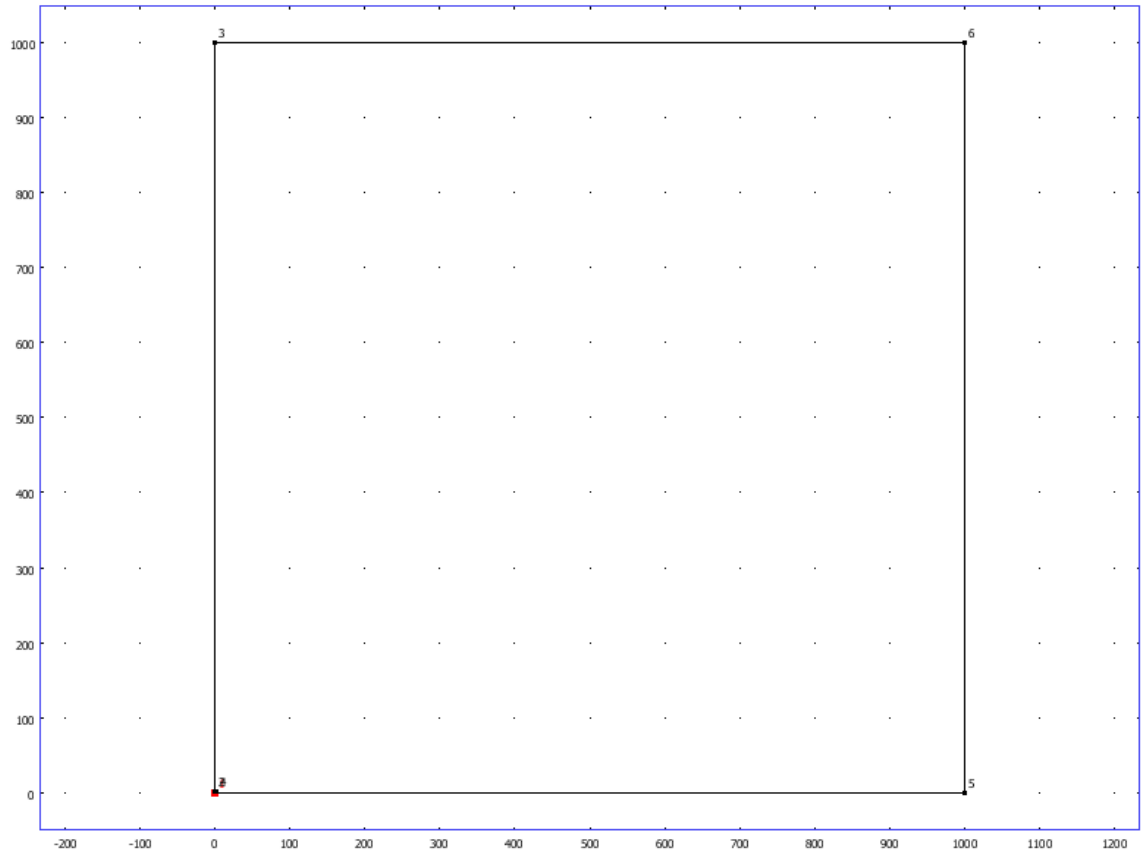

3.1.2. Boundary mode

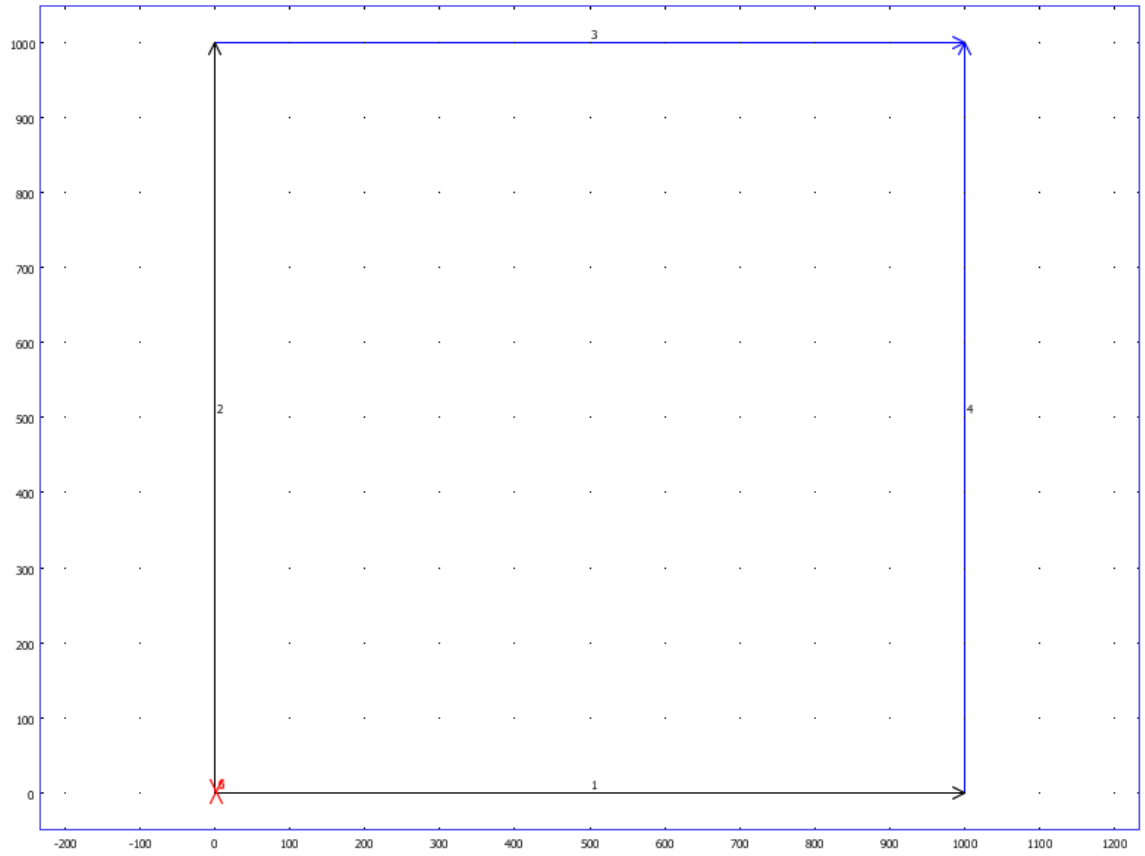

3.1.3. Subdomain mode

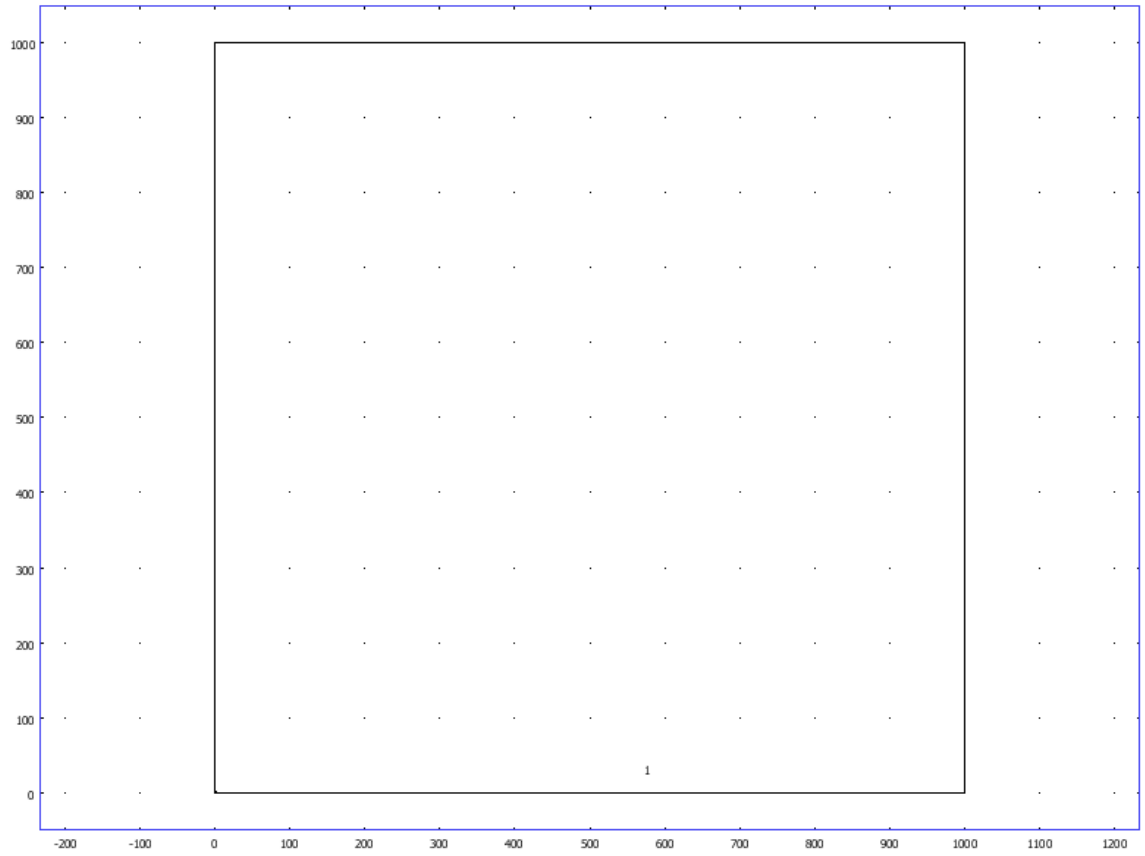

4. Geom1

Space dimensions: 2D

Independent variables: x, y, z

4.1. Mesh

4.1.1. Mesh Statistics

Number of degrees of freedom	10333
Number of mesh points	2710
Number of elements	4914
Triangular	4914

Quadrilateral	0
Number of boundary elements	504
Number of vertex elements	6
Minimum element quality	0.005
Element area ratio	0

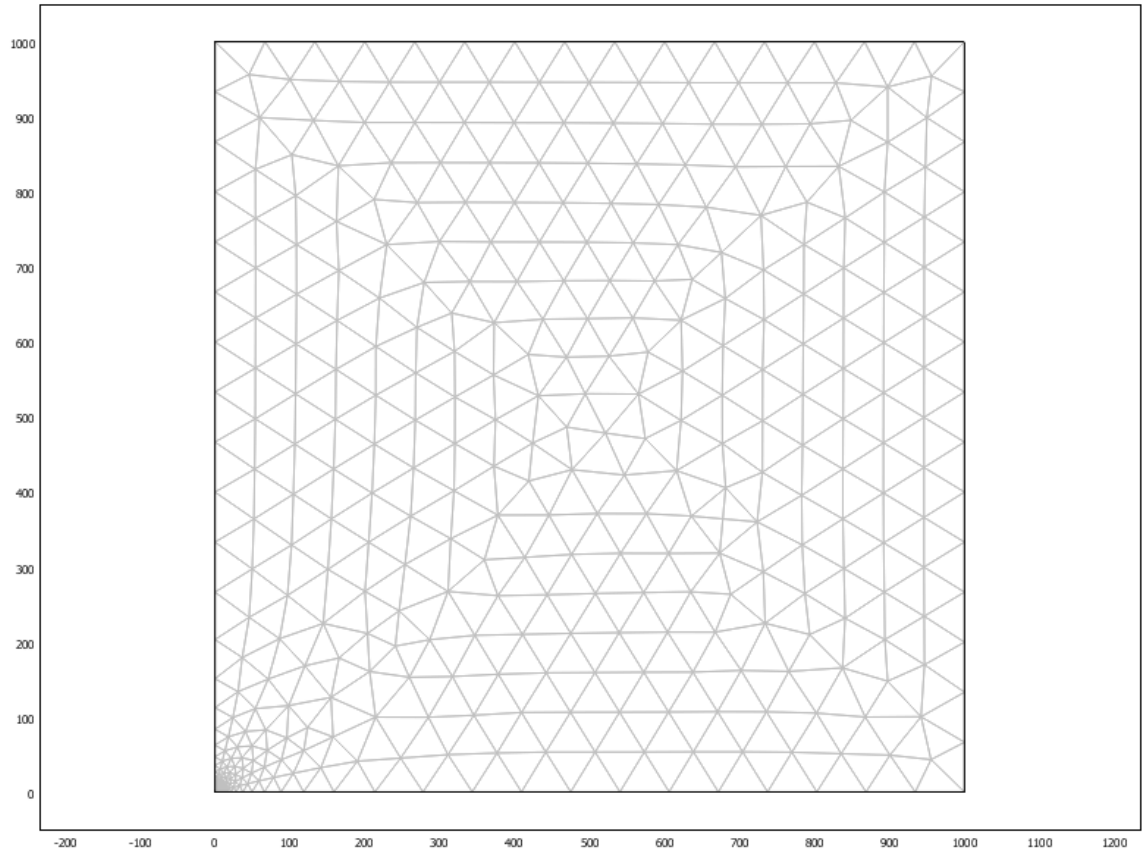

4.2. Application Mode: Diffusion (chdi)

Application mode type: Diffusion (Chemical Engineering Module)

Application mode name: chdi

4.2.1. Application Mode Properties

Property	**Value**

Default element type	Lagrange - Quadratic
Analysis type	Stationary
Equilibrium assumption	Off
Frame	Frame (ref)
Weak constraints	Off
Constraint type	Ideal

4.2.2. Variables

Dependent variables: c

Shape functions: shlag(2,'c')

Interior boundaries not active

4.2.3. Boundary Settings

Boundary		1-2	3-4	5-6
Type		Insulation/Symmetry	Concentration	Flux
Mass transfer coefficient (kc)	m/s	0	0	**10**
Concentration (c0)	mol/m^3	0	**1**	0

4.2.4. Subdomain Settings

The subdomain settings only contain default values.

Subdomain initial value		1
Concentration, c (c)	mol/m^3	1

5. Solver Settings

Solve using a script: off

Analysis type	Stationary

Auto select solver	On
Solver	Stationary
Solution form	Automatic
Symmetric	auto
Adaptive mesh refinement	Off
Optimization/Sensitivity	Off
Plot while solving	Off

5.1. Direct (UMFPACK)

Solver type: Linear system solver

Parameter	**Value**
Pivot threshold	0.1
Memory allocation factor	0.7

5.2. Stationary

Parameter	**Value**
Linearity	Automatic
Relative tolerance	1.0E-7
Maximum number of iterations	25
Manual tuning of damping parameters	Off
Highly nonlinear problem	Off
Initial damping factor	1.0
Minimum damping factor	1.0E-4
Restriction for step size update	10.0

5.3. Advanced

Parameter	Value
Constraint handling method	Elimination
Null-space function	Automatic
Automatic assembly block size	On
Assembly block size	1000
Use Hermitian transpose of constraint matrix and in symmetry detection	Off
Use complex functions with real input	Off
Stop if error due to undefined operation	On
Store solution on file	Off
Type of scaling	Automatic
Manual scaling	
Row equilibration	On
Manual control of reassembly	Off
Load constant	On
Constraint constant	On
Mass constant	On
Damping (mass) constant	On
Jacobian constant	On
Constraint Jacobian constant	On

6. Postprocessing

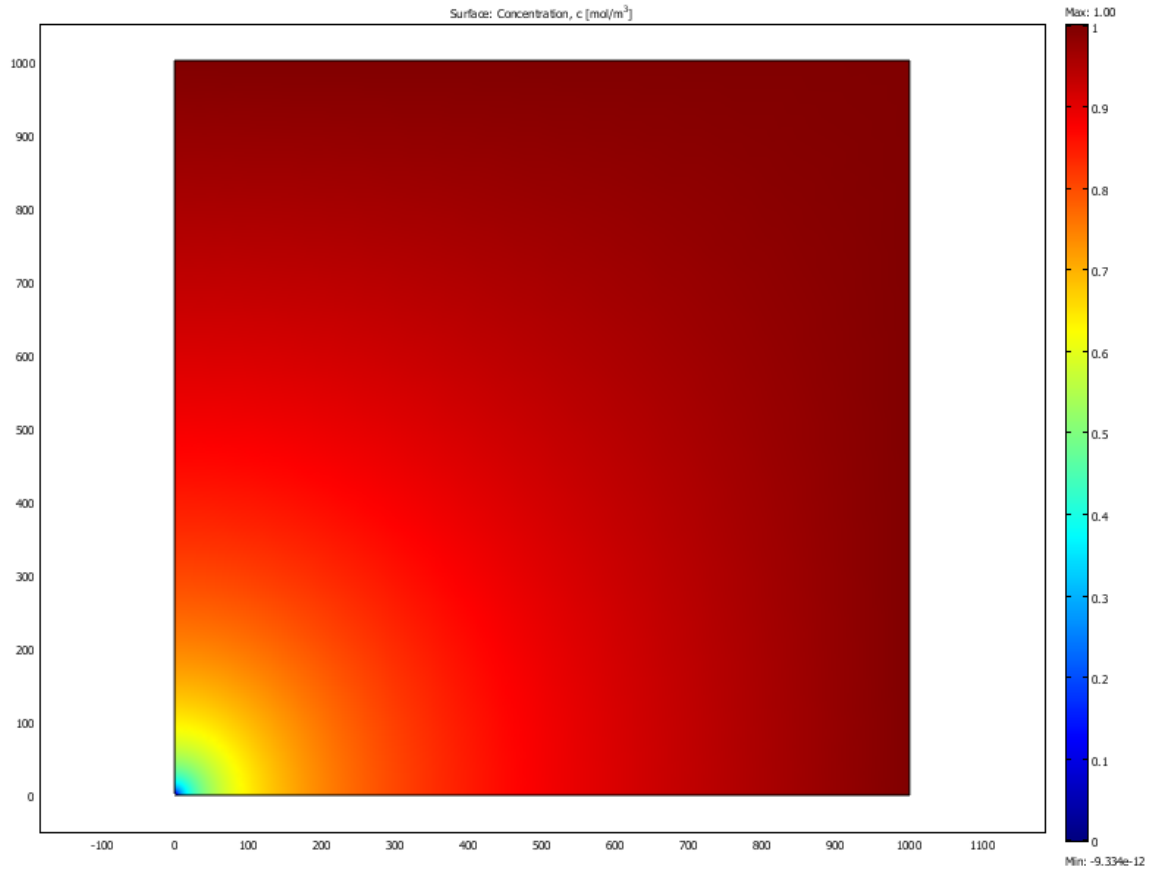

7. Variables

7.1. Boundary

Name	Description	Unit	Expression
ndflux_c_chdi	Normal diffusive flux, c	mol/(m^2*s)	nx_chdi * dflux_c_x_chdi+ny_chdi * dflux_c_y_chdi

7.2. Subdomain

Name	Description	Unit	Expression
grad_c_x_chdi	Concentration gradient, c, x component	mol/m^4	cx

dflux_c_x_chdi	Diffusive flux, c, x component	mol/(m^2*s)	-Dxx_c_chdi * cx-Dxy_c_chdi * cy
grad_c_y_chdi	Concentration gradient, c, y component	mol/m^4	cy
dflux_c_y_chdi	Diffusive flux, c, y component	mol/(m^2*s)	-Dyx_c_chdi * cx-Dyy_c_chdi * cy
grad_c_chdi	Concentration gradient, c	mol/m^4	sqrt(grad_c_x_chdi^2+grad_c_y_chdi^2)
dflux_c_chdi	Diffusive flux, c	mol/(m^2*s)	sqrt(dflux_c_x_chdi^2+dflux_c_y_chdi^2)